Thin Solid Films 519 (2011) 4963–4968

Contents lists available at ScienceDirect

Thin Solid Films

journal homepage: www.elsevier.com/locate/tsf

The effect of titanium current on structure and hardness of aluminium titanium nitride deposited by reactive unbalanced magnetron co-sputtering

A. Buranawong [a,c,*], N. Witit-anun [b,c], S. Chaiyakun [b,c], A. Pokaipisit [a,c], P. Limsuwan [a,c]

[a] Department of Physics, Faculty of Science, King Mongkut's University of Technology Thonburi, 126 Pracha-utid Road, Bangmod, Toongkru, Bangkok,10140, Thailand
[b] Department of Physics, Faculty of Science, Burapha University, 169 Long-Hard Bangsaen Road, Saen Sook, Chonburi, 20131, Thailand
[c] Thailand Center of Excellence in Physics, CHE, Ministry of Education, Bangkok 10400, Thailand

ARTICLE INFO

Available online 14 January 2011

Keywords:
Titanium current
Aluminium titanium nitride
Reactive magnetron co-sputtering

ABSTRACT

Nanocrystalline aluminium titanium nitride ($AlTi_3N$) thin films were deposited on Si (100) wafer and grid substrates without external heating and biasing at room temperature by reactive unbalanced magnetron co-sputtering technique using pure individual titanium and aluminium targets. The effects of titanium current (I_{Ti}) on the structure and hardness of these films have been studied. The films were sputtered with Ar and N_2 gases flow rate of 8 and 4 sccm, respectively. The sputtering current of the aluminium current (I_{Al}) was kept at 600 mA and the sputtering current of titanium (I_{Ti}) was varied from 600 to 800 mA. The films were deposited for different deposition times ranging from 15 to 60 min. The deposited films were then characterized and analyzed by X-Ray Diffraction (XRD), Atomic Force Microscopy (AFM), Scanning Electron Microscopy (SEM), Transmission Electron Microscopy (TEM) and nanoindentation measurement. The results indicated that the modification of the crystal structure, surface morphology and microstructure were dependent on the deposition parameters. The XRD patterns show polycrystalline structure with preferred orientations in (112), (004) and (153) planes which agree with the standard structure of aluminium titanium nitride ($AlTi_3N$) films. In addition, the structure of $AlTi_3N$ was also confirmed by TEM. These results show that the films are composed of high Al content. The root mean square surface roughness and the average thicknesses were strongly influenced by I_{ti} and deposition times. Cross section analysis by SEM showed dense and compact columnar morphology. The typical hardness of the films was approximately 26.24–30.37 GPa.

1. Introduction

Binary nitride films such as TiN films are widely used in many industrial applications in the past decades owing to their high hardness, good wear resistance, good corrosion resistance, and long lifetime [1,2]. Therefore, machining tools such as drills, hobs, mills and cutting tools are extensively deposited with titanium nitride (TiN) because of its hardness of approximately 20 GPa. Moreover, due to its gold-like appearance it is widely used for decorative coating [3,4]. However, the disadvantage of TiN is that it is oxidized rapidly at temperatures above about 500 °C which can occur during machining process [4,5]. Therefore, the incorporation of aluminium addition in a form of solid solution ternary nitride of TiAlN was developed to replace TiN since it demonstrates outstanding physical, mechanical, and tribological properties. This includes high hardness values, low wear, high corrosion resistance and excellent oxidation resistance at elevated temperature of 700 °C [6] that is higher than that of TiN. Furthermore, hard and stable aluminium oxide (Al_2O_3) layer can be formed for the underlying coating when the high speed cutting environment (≥600 °C) is required [7,8].

Various methods were used to deposit the TiAlN thin films including chemical vapor deposition [9], cathodic arc vapor deposition [10], reactive magnetron sputtering [2,17], etc. Among them, sputtering technique is the most suitable one due to low-temperature processing, use of non toxic gases and simple deposition process [8]. Generally, if the films compose of Al more than 50%, it is called "aluminium titanium nitride" [11]. Nevertheless, although the deposition parameters will effect to the properties of the coating, the relationship between TiAlN prepared at different titanium currents on crystal structure, surface morphology and microstructure have not been sufficiently investigated.

However, the structure and variety of TiAlN thin film prepared by sputtering under different deposition conditions have been widely studied, most of them were prepared at short target to substrate distance [12,13], applied bias voltage [4,14], high current of targets [15] and substrate heating [16] to reach good crystal structure.

Since the sputter yield of titanium is 0.5 lower than that of aluminium (1.0), hence the aluminium atom can be easily sputtered from the target. The method to reach the stoichiometry $Ti_{1-x}Al_xN$ is to apply high current to the titanium target compared to the aluminium

* Corresponding author. Department of Physics, Faculty of Science, King Mongkut's University of Technology Thonburi, 126 Pracha-utid Road, Bangmod, Toongkru, Bangkok, 10140, Thailand.
E-mail address: a.buranawong@gmail.com (A. Buranawong).

0040-6090/$ – see front matter.
doi:10.1016/j.tsf.2011.01.062

Table 1
Deposition condition of $AlTi_3N$ thin film.

Deposition parameters	Details
Target	Titanium (99.97%), aluminium (99.999%)
Base pressure (mbar)	5.0×10^{-5} mbar
Total pressure (mbar)	5.0×10^{-3} mbar
Substrate	Silicon wafer, glass slide, copper grid
Ar flow rate (sccm)	8
N_2 flow rate (sccm)	4
Titanium current (mA)	600, 700, 800
Aluminium current (mA)	600
Deposition time (min)	15, 30, 45, 60
Target to substrate distance (cm)	13

target that was used. The objective of this research is to prepare nanocrystalline $AlTi_3N$ thin films on unheated substrates and long target-to-substrate distance by reactive magnetron co-sputtering from pure Ti and Al targets.

2. Experiment

The $AlTi_3N$ thin films were deposited on both silicon wafer (100) and copper grid without external heating by a home-made reactive magnetron co-sputtering system as shown in Fig. 1. The substrates were ultrasonically cleaned in trichloroethylene, acetone and isopropyl alcohol by ultrasonic for 10 min each sequentially and then dried before installation into the vacuum chamber. The films were prepared by high purity titanium (99.97%) and aluminium (99.999%) of 3 in. in diameter and a thickness of 0.125 in. in a mixture of high purity argon (99.999%) and nitrogen (99.999%) atmosphere. A diffusion pump accompanied with rotary pump was used to achieve the base pressure of 5.0×10^{-5} mbar. Prior to each deposition, the targets were presputtered for 5 min in order to remove the contaminants from the target's surface. The total pressure was kept constant at 5.0×10^{-3} mbar with Ar and N_2 constant gas flow rates of 8 to 4 sccm. In the deposition process, all the films were carried out at long target to substrate a distance of 13 cm with a constant aluminium current of 600 mA and different titanium currents from 600 to 800 mA. For each titanium current, the films were deposited for various times of 15, 30, 45 and 60 min as show in Table 1.

The crystal structure of the films was characterized by x-ray diffractometer (Riguku, Rint 2000) using Cu Kα radiation operated at 40 kV and 40 mA with a glazing incidence angle (3°). The 2θ was scanned from 20°–65° and a scanning speed of 2°/min. The surface morphology, roughness and thickness were observed by an atomic force microscope (Nanoscope IV, Veeco Instrument Inc). The scan area was carried out in an area of $1\times1\ \mu m^2$. The structure of the films was also analyzed using TEM (JEOL TEM-2001). The cross-section morphology was investigated by field emission scanning electron microscope (FE-SEM, Hitachi S-4700). The hardness of the films was measured by a nanoidentator (HYSITRON TriboIndenter Model TI-900).

3. Results and discussions

3.1. The influence of deposition times on crystal structure

Fig. 2 shows the XRD patterns of the films deposited at a titanium current (I_{Ti}) of 600 mA for various deposition times from 15 to 60 min. It revealed that the films exhibited preferred orientations of (112), (004) and (153) planes at 2θ of 36.78°, 42.96° and 62.44°, respectively. According to standard JCPDS file number 51-0724, the deposited films obtained are of the orthorhombic $AlTi_3N$ structures. In addition, (100) plane at 2θ of 56.5° was identified as the silicon substrate. The same characteristic peaks appeared for all deposition times. At a deposition time of 30 min, the x-ray intensity of (004) plane was highest compared to the other peaks.

When increasing the deposition time to 45 min, it revealed that the x-ray intensity of (112) and (153) peaks increases significantly but the reverse trend was observed for (004) plane. The x-ray diffraction patterns of the films deposited for 60 min also exhibited a diffraction peak of $AlTi_3N$ (112), (004) and (153) planes, respectively. It was clearly observed that smaller peak at (004) plane was observed compared to the films deposited for a shorter deposition time. The decrease of x-ray intensities was observed for the (112) plane however it was observed to have the highest x-ray intensity.

By comparing the XRD pattern of each deposition time, it is noted that the crystal structure was significantly developed with the longer deposition time and showed a high Al composition in the films achieved from our experiment using the reactive magnetron co-sputtering system. The XRD intensity of the preferred orientation in the (112)

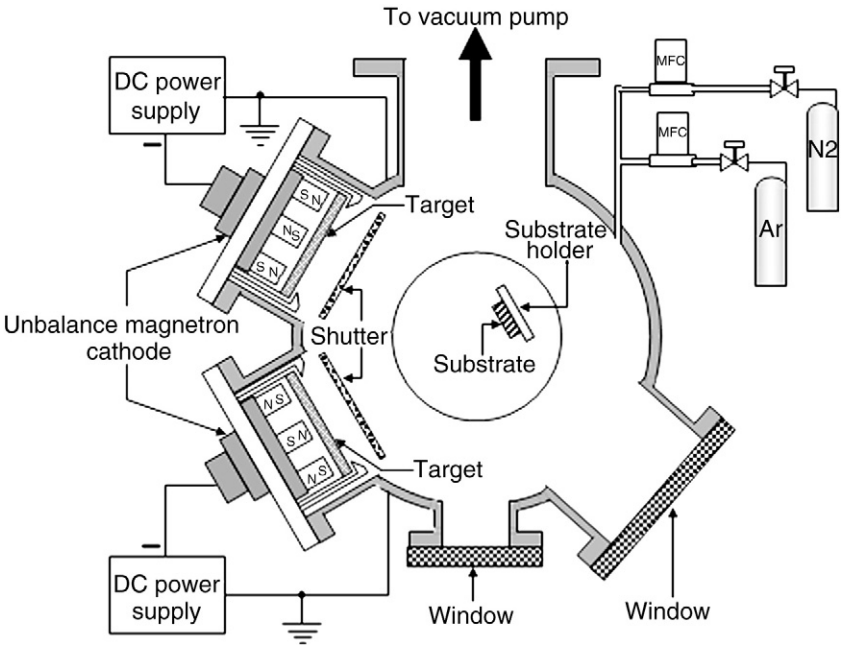

Fig. 1. Schematic diagram of the reactive magnetron co-sputtering system.

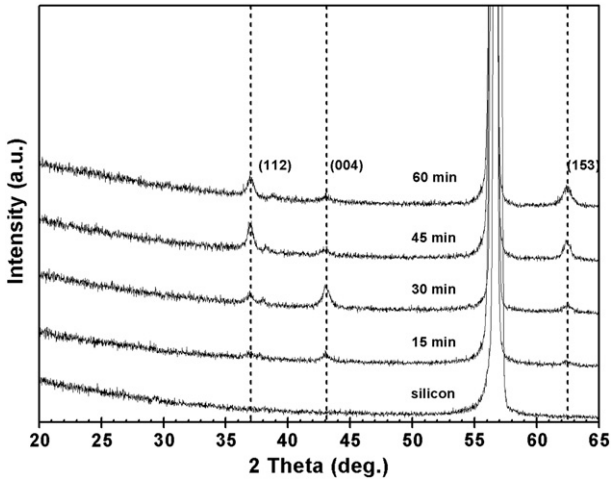

Fig. 2. The XRD patterns of $AlTi_3N$ thin films deposited with I_{Ti} 600 mA and I_{Al} 600 mA for different deposition times.

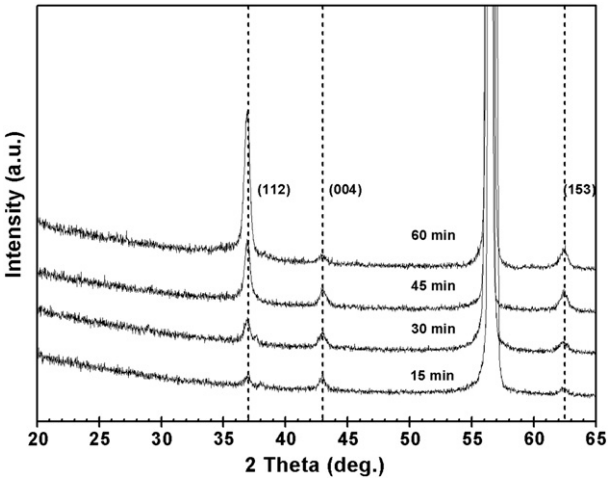

Fig. 4. The XRD patterns of $AlTi_3N$ thin films deposited with I_{Ti} 800 mA and I_{Al} 600 mA for different deposition times.

and (153) planes was developed. The increasing and decreasing of (112) plane were observed whereas there was only the increasing in (153) plane over the deposition time. The peak intensity with significant increase and decrease was investigated for the (004) plane. The change of x-ray intensity was attributed to the higher amount of titanium atoms from the sputtered target which increases adatom mobility during film formation and leads to higher crystallinity of the films through longer deposition time [17].

Figs. 3 and 4 show XRD patterns of the films deposited at I_{Ti} of 700 and 800 mA, respectively. The XRD results show the similar crystal structure development to the case when I_{Ti} was 600 mA over the deposition time. It is seen that the x-ray intensities of (112), (004) and (153) planes all increased for the films deposited with longer deposition time. The results revealed that the increased crystallinity of structure was assisted by atoms with higher energy, therefore, higher mobility to form crystal in preferred orientations.

The influence of I_{Ti} on crystal structure was further investigated. Fig. 5 shows the XRD patterns of the films deposited at I_{Ti} of 600, 700 and 800 mA for a deposition time of 60 min. It is seen that the intensity of (112) plane rapidly increased compared to the (004) and (153) planes. The higher crystallinity due to the increase of I_{ti} is related to high energy particles received from higher current applied to the titanium target. It can be concluded, by XRD results, that the films prepared in this work indicated certain composition of $AlTi_3N$ structure which implied that the films exhibit the $AlTi_3N$ compound structure under the current deposition conditions due to sufficient Al amount added to form compounds of different phases of $Ti_{1-x}Al_xN$ according to x value [18].

3.2. The surface morphology

The AFM images of surface morphology of the coatings are shown in Fig. 6 with three-dimensional representations (1 μm × 1 μm surface plots), corresponding to the samples prepared with a titanium current of 600 to 800 mA while the aluminium current was fixed at 600 mA and for 60 min of deposition time for all films. At a titanium current of 600 mA, the nanocrystalline $AlTi_3N$ grains were formed mainly of individual grain and compact pattern which are clearly identified (Fig. 6a). The aggregation of some grains to form the bigger triangle shape grains were observed for the films deposited with 700 mA. In addition, the aggregation of grains are also arranged throughout the surface with larger size, denser structure and obviously more separated individual grain (Fig. 6b). The nanocrystalline grains of the film deposited with 800 mA of titanium current formed triangle shapes with porous morphology and spreading across the surface as shown in Fig. 6c. The surface roughnesses of the three sample surfaces shown in

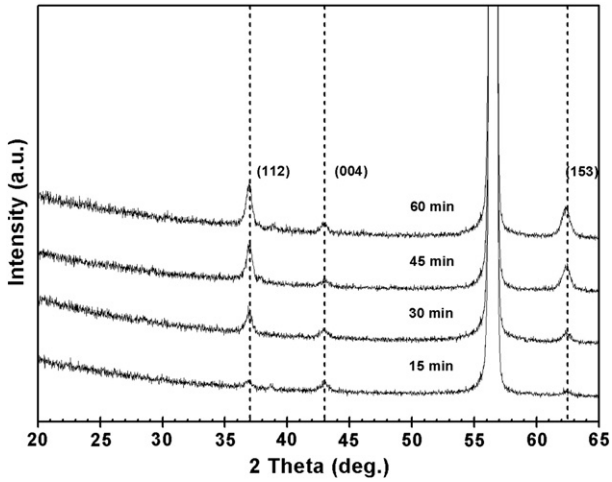

Fig. 3. The XRD patterns of $AlTi_3N$ thin films deposited with I_{Ti} 700 mA and I_{Al} 600 mA for different deposition times.

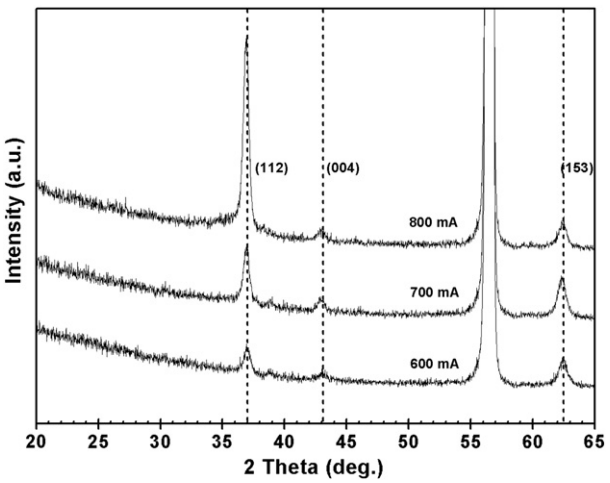

Fig. 5. The XRD patterns of $AlTi_3N$ thin films deposited by varying titanium current (I_{Ti}) for the same deposition time of 60 min.

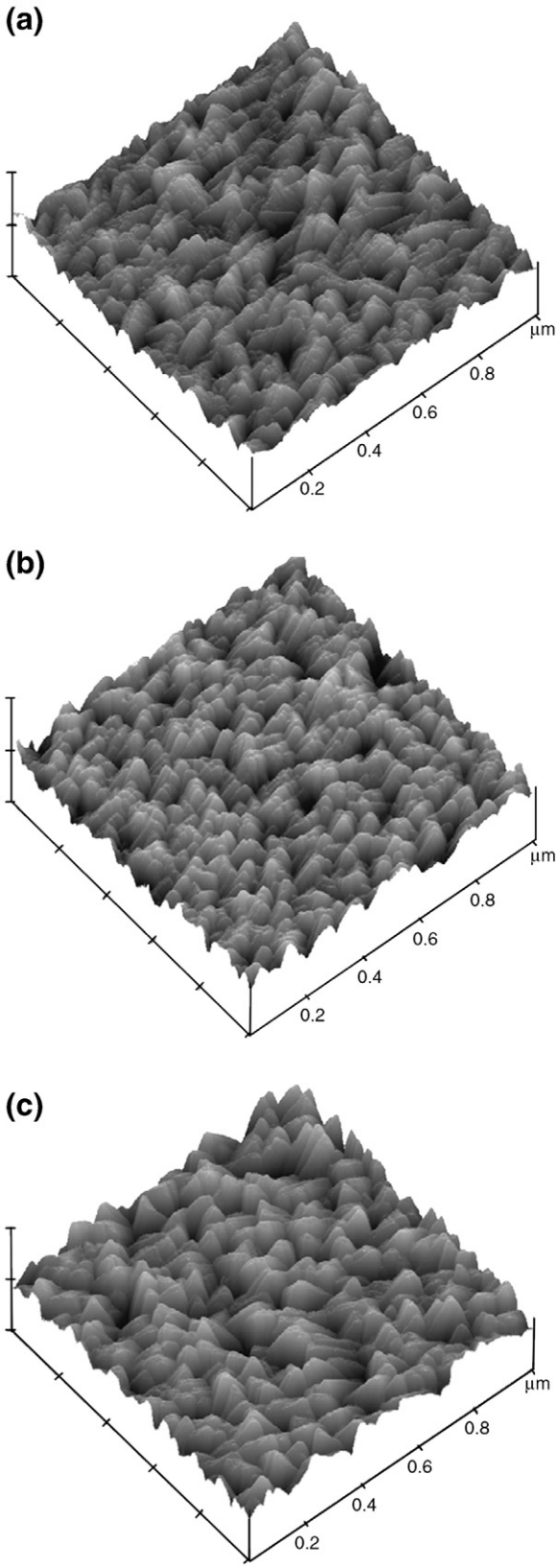

Fig. 6. The AFM images of $AlTi_3N$ thin films deposited by varying titanium current (I_{Ti}) for the same deposition time of 60 min.

Fig. 6a–c were found to be 9.0, 11.0 and 17.4 nm, respectively. Similar results were also obtained for deposition times of 15, 30 and 45 min, and the results on the surface roughness are shown in Table 2. It is seen that the average grain size and average film thickness increases with increasing deposition time and increasing titanium current as shown in Tables 2 and 3. It is found that the average film thickness varied from a minimum value of 141.7 nm to a maximum value of 1184.7 nm.

Table 2
Variations of average surface roughness and the grain size of $AlTi_3N$ film with four different deposition times and three different titanium currents of 600, 700 and 800 mA.

Deposition time (min)	Average rms roughness (nm)			Average grain size (nm)		
	600 mA	700 mA	800 mA	600 mA	700 mA	800 mA
15	1.8	2.0	4.1	13.7	21.6	49.8
30	2.0	2.7	7.6	13.7	64.7	75.2
45	5.9	7.0	13.7	14.7	73.5	81.1
60	9.0	11.0	17.4	19.6	90.2	125.1

The surface morphology evolution was related to the enhancement of atom energy from the increasing of titanium current that resulted not only to larger grain size and less dense grain, but also affected the thickness of the films as the increasing of titanium current will generate more Ti particles off the target and readily form the structure.

3.3. The microstructure

The cross-sectional observations from Fig. 7 indicate that the films have columnar structure. However, the columnar structure exhibited some changes when the deposition time is varied while the deposited current was fixed at a titanium current of 800 mA and an aluminium current of 600 mA. The surface morphology of the sample deposited for 15 min as shown in Fig. 8a apparently reveals the equiaxial structure. The films also exhibit good columnar pattern and each individual grain can be observed for 30 min, as shown in Fig. 7b. The films prepared at the higher deposition times of 45 and 60 min (Fig. 7c and d) show individual grain clearly with columnar characteristic and have more open boundaries such as pores or void through the surface between columns than for denser films prepared for shorter deposition times (15 and 30 min). In addition, it is noticed that the films grow continuously along the deposition time as indicated by the thickness measurement from the cross-section analysis of SEM images. When the applied current on the titanium target is further increased, the denser packing of the grain column was the result of the incoming atom on the surface with features similar to the zone 2 microstructure according to the Thornton's model [19].

The structure of $AlTi_3N$ films was investigated by TEM. Fig. 8a shows a typical plane view of high-resolution transmission electron microscopy (HRTEM) image of a film deposited for 60 min. According to the HRTEM image, the lattice fringes are clearly distinguished and the measured distance of the fringe was 0.24 nm which is in a good agreement with the standard JCPDS:51-0724 of the (112) plane with a d value of 0.24 nm for the $AlTi_3N$ orthorhombic phase. The related SAED pattern of the $AlTi_3N$ films is shown in Fig. 8b. The (112), (004) and (153) diffraction rings of the orthorhombic structure correspond to the nanocrystalline $AlTi_3N$ from the standard data (JCPDS:51-0724). The results from TEM measurement not only can evidently

Table 3
Variations of average thickness and the grain size of $AlTi_3N$ Film with four different deposition times and three different titanium currents of 600, 700 and 800 mA.

Deposition time (min)	Film thickness (nm)		
	600 mA	700 mA	800 mA
15	141.74	183.79	255.19
30	265.61	353.31	468.98
45	416.24	568.31	906.18
60	581.90	823.54	1184.67

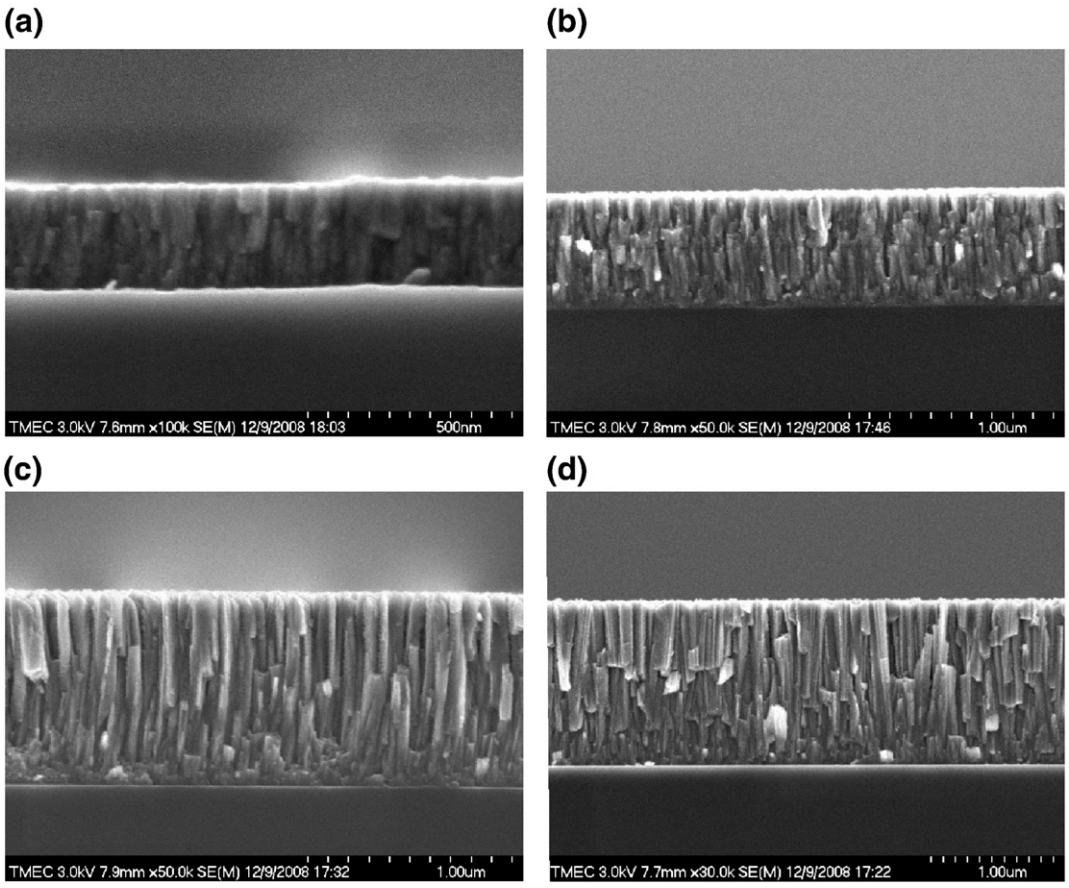

Fig. 7. The cross-section morphology of $AlTi_3N$ thin films from the different deposition times (a) 15 min, (b) 30 min, (c) 45 min and (d) 60 min at a titanium current of 800 mA.

conclude with a good agreement to the standard data of $AlTi_3N$, but also able to confirm the crystal structure from the XRD results.

3.4. The microhardness

The hardness values of $AlTi_3N$ which are obtained from the nanoindentation technique were in the range of 26.24–30.37 GPa. The hardness increased with increasing titanium current. The hardness enhancement is mainly due to the increase of the nanocomposite and individual columnar of the $AlTi_3N$ thin film which has a dense structure.

4. Conclusion

Nanocrystalline aluminium titanium nitride ($AlTi_3N$) thin films were successfully deposited at room temperature by reactive magnetron co-

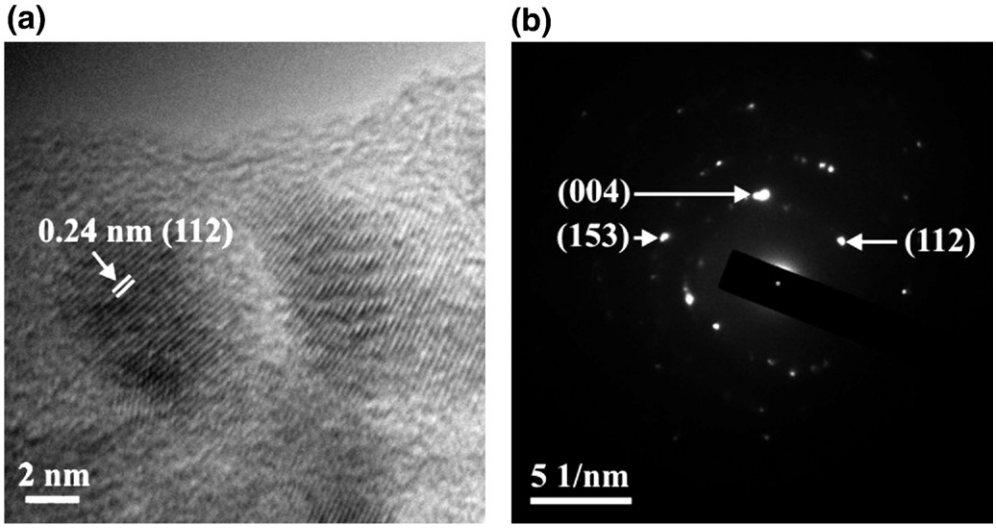

Fig. 8. (a) HRTEM image of $AlTi_3N$ film and (b) SAED image of $AlTi_3N$ film deposited at 60 min.

sputtering technique. The crystal structure, the surface morphology and microstructure are strongly influenced by deposition time. The $AlTi_3N$ (112), (004) and (153) planes were obtained. The crystallinity of $AlTi_3N$ films increased with increasing titanium current and deposition time. It was found that the grain size, the surface roughness and the average thicknesses of the films were increased by varied titanium current and deposition times. The films exhibited columnar and dense structure observed by SEM technique. Further investigation concerning the confirmation of $AlTi_3N$ structure using TEM analysis showed a good agreement with XRD results. In addition, the hardness was in the range of 26.24–30.37 GPa.

Acknowledgments

A. Buranawong would like to thank the Commission on Higher Education, Thailand for supporting by a grant fund under the program Strategic Scholarships for Frontier Research Network for the Ph.D. Program Thai Doctoral degree for this research. The authors would like to thank Vacuum Technology and Thin Films Research Laboratory, Burapha University for providing the sputtering facilities. This work was partly funded by KMUTT under the National Research University Project.

References

[1] G.T. Liu, J.G. Duh, K.H. Chung, J.H. Wang, Surf. Coat. Technol. 200 (2005) 2001.
[2] J.C. Oliveria, A. Manaia, J.P. Dias, A. Cavalerio, D. Teer, S. Taylor, Surf. Coat. Technol. 200 (2006) 6583.
[3] S.H. Ahn, J.H. Hong, J.G. Kim, J.G. Han, Thin Solid Films 515 (2007) 6878.
[4] K. Chu, P.W. Shum, Y.G. Chen, Mater. Sci. Eng. B. 131 (2006) 62.
[5] R. Wuhrer, W.Y. Yeung, Scr. Mater. 50 (2004) 813.
[6] H.C. Barshilia, K. Yogesh, K. Rajam, Vacuum 83 (2009) 427.
[7] J.T. Chen, J. Wang, F. Zhang, G.A. Zhang, X.Y. Fan, Z.G. Wu, P.X. Yan, J. Alloy. Compd. 472 (2009) 91.
[8] P.W. Shum, K.Y. Li, Y.G. Shen, Surf. Coat. Technol. 198 (2004) 414.
[9] J. Wagner, V. Eldlmayr, M. Penoy, C. Michottle, C. Mitterer, M. Kathrein, Int. J. Refract. Met. Hard Mater. 26 (2008) 563.
[10] S. Paldey, S.C. Deevi, Mater. Sci. Eng. B. 361 (2003) 1.
[11] S. Surinpong, technique 198 (2002) 122.
[12] R. Wuhrer, W.Y. Yeung, Scr. Mater. 49 (2003) 200.
[13] K.H. Chung, G.T. Liu, J.G. Duh, J.H. Wang, Surf. Coat. Technol. 188–189 (2004) 746.
[14] Z.J. Liu, P.W. Shum, Y.G. Shen, Thin Solid Films 496 (2006) 327.
[15] J.C. Oliveira, A. Manaia, A. Cavaleiro, Thin Solid Films 516 (2008) 5033.
[16] B. Subramanian, K. Ashok, P. Kuppusami, C. Sanjeeviraja, M. Jayachandran, Cryst. Res. Technol. 43 (2008) 1079.
[17] A. Buranawong, S. Chaiyakhun, P. Limsuwan, Adv. Mater. Res. 93–94 (2010) 341.
[18] J. Musil, H. Hrubý, Thin Solid Films 365 (2000) 104.
[19] R. Wuhrer, W.Y. Yeung, J. Mater. Sci. 37 (2002) 3479.